Cholecystokinin 2 Receptor Agonist ^{177}Lu-PP-F11N for Radionuclide Therapy of Medullary Thyroid Carcinoma: Results of the Lumed Phase 0a Study

Christof Rottenburger*[1], Guillaume P. Nicolas*[1,2], Lisa McDougall[1], Felix Kaul[1,2], Michal Cachovan[3], A. Hans Vija[4], Roger Schibli[5], Susanne Geistlich[6], Anne Schumann[7], Tilman Rau[8], Katharina Glatz[9], Martin Behe[6], Emanuel R. Christ[2,10], and Damian Wild[1,2]

[1]Division of Nuclear Medicine, University Hospital Basel, Basel, Switzerland; [2]Center for Neuroendocrine and Endocrine Tumors, University Hospital Basel, Basel, Switzerland; [3]Siemens Healthcare GmbH, Forchheim, Germany; [4]Molecular Imaging, Siemens Medical Solutions USA, Inc., Hoffman Estates, Illinois; [5]Department of Chemistry and Applied Biosciences, Institute of Pharmaceutical Sciences, ETH, Zurich, Switzerland; [6]Center for Radiopharmaceutical Sciences, Paul Scherrer Institute, Villigen, Switzerland; [7]3B Pharmaceuticals GmbH, Berlin, Germany; [8]Institute of Pathology, University of Bern, Bern, Switzerland; [9]Institute of Pathology, University Hospital Basel, Basel, Switzerland; and [10]Division of Endocrinology, Diabetology and Metabolism, University Hospital Basel, Basel, Switzerland

Treatment of patients with advanced medullary thyroid carcinoma (MTC) is still a challenge. For more than 2 decades, it has been known that the cholecystokinin 2 receptor is a promising target for the treatment of MTC with radiolabeled minigastrin analogs. Unfortunately, kidney toxicity has precluded their therapeutic application so far. In 6 consecutive patients, we evaluated with advanced 3-dimensional dosimetry whether improved minigastrin analog ^{177}Lu-DOTA-(D-Glu)$_6$-Ala-Tyr-Gly-Trp-Nle-Asp-PheNH$_2$ (^{177}Lu-PP-F11N) is a suitable agent for the treatment of MTC. **Methods:** Patients received 2 injections of about 1 GBq (~80 μg) of ^{177}Lu-PP-F11N with and without a solution of succinylated gelatin (SG, a plasma expander used for nephroprotection) in a random crossover sequence to evaluate biodistribution, pharmacokinetics, and tumor and organ dosimetry. An electrocardiogram was obtained and blood count and blood chemistry were measured up to 12 wk after the administration of ^{177}Lu-PP-F11N to assess safety. **Results:** In all patients, ^{177}Lu-PP-F11N accumulation was visible in tumor tissue, stomach, and kidneys. Altogether, 13 tumors were eligible for dosimetry. The median absorbed doses for tumors, stomach, kidneys, and bone marrow were 0.88 (interquartile range [IQR]: 0.85–1.04), 0.42 (IQR: 0.25–1.01), 0.11 (IQR: 0.07–0.13), and 0.028 (IQR: 0.026–0.034) Gy/GBq, respectively. These doses resulted in median tumor-to-kidney dose ratios of 11.6 (IQR: 8.11–14.4) without SG and 13.0 (IQR: 10.2–18.6) with SG; these values were not significantly different ($P = 1.0$). The median tumor-to-stomach dose ratio was 3.34 (IQR: 1.14–4.70). Adverse reactions (mainly hypotension, flushing, and hypokalemia) were self-limiting and not higher than grade 1. **Conclusion:** ^{177}Lu-PP-F11N accumulates specifically in MTC at a dose that is sufficient for a therapeutic approach. With a low kidney and bone marrow radiation dose, ^{177}Lu-PP-F11N shows a promising biodistribution. The dose-limiting organ is most likely the stomach. Further clinical studies are necessary to evaluate the maximum tolerated dose and the efficacy of ^{177}Lu-PP-F11N.

According to recent data from the Surveillance, Epidemiology, and End Results database, medullary thyroid cancer (MTC) represents 1%–2% of all thyroid cancers in the United States. Distant metastases can be detected clinically in 4%–17% of patients at the time of diagnosis (1,2). MTC lacks the accumulation of radioactive iodine, and cytotoxic chemotherapy has shown disappointing results for advanced MTC (1). The kinase inhibitors vandetanib and cabozantinib are approved for the treatment of MTC (3,4) but have not shown a significant effect on overall survival and may cause significant adverse reactions, including QT prolongation. Radionuclide therapy with compounds such as ^{90}Y-DOTATOC and ^{131}I pretargeted anticarcinoembryonic antigen radioimmunotherapy were described in 2006 and 2007, with promising results (5,6). However, they have not been introduced into clinical routines so far. Therefore, there is an unmet need for a more effective systemic therapy for patients with advanced MTC.

Specific targeting of MTC cells with radiolabeled minigastrin analogs has the potential to improve imaging and to allow peptide receptor radionuclide therapy, as greater than 90% of MTCs express the transmembrane G protein–coupled cholecystokinin 2 receptor (CCK2R) at a high density (7). Eight patients with advanced MTC were treated in a pilot study with the CCK2R-specific ^{90}Y-labeled minigastrin analog diethylaminetriaminepentaacetic acid (DTPA)-Glu$_1$-minigastrin (8). This treatment resulted in partial remission in 4 patients and stable disease in 2 patients, lasting for up to 36 mo. Unfortunately, nephrotoxicity and bone marrow toxicity limited the therapeutic application of this first radiolabeled minigastrin analog.

Coinjection of nephroprotective substances is often used to reduce nephrotoxicity. This approach (with a 4% succinylated gelatin solution [SG], which has an international marketing authorization for use as a

plasma expander [Gelofusine; B. Braun Medical AG]) was evaluated in rats and showed promising results. SG resulted in a 45% reduction in the renal cortex uptake of ^{111}In-DTPA-Glu$_1$-minigastrin (9), whereas the cationic amino acid lysine did not show a significant effect. Another approach for reducing nephrotoxicity is modification of the compound itself; amino acid chains with more than 5 glutamic acids in their sequence play an important role in the kidney reuptake mechanism and may reduce kidney uptake (10,11). Such an approach was implemented by several groups and resulted in the development of a library of improved radiolabeled minigastrin analogs (12–17). Some of these new compounds show higher tumor uptake, higher tumor-to-kidney uptake ratios, and higher serum stability than previously developed minigastrin analogs. One of the most promising new compounds is PP-F11N [DOTA-(D-Glu)$_6$-Ala-Tyr-Gly-Trp-Nle-Asp-PheNH$_2$], which can be labeled with ^{177}Lu, a widely used radionuclide that has not only excellent therapeutic properties but also a γ-ray component that allows the acquisition of good-quality images for a personalized treatment approach (theranostics) as well as dosimetry studies (16).

Here, to the best of our knowledge, we present the first-in-humans results for ^{177}Lu-PP-F11N. The primary endpoint was the proof of CCK2R-specific in vivo targeting and visualization of MTC metastases in correlation with histology, in vitro autoradiography, or ^{18}F-dihydroxyphenylalanine (DOPA) PET/CT as a standard of comparison. Secondary endpoints were safety, biodistribution, pharmacokinetics, and radiation dosimetry after the injection of a test dose of ^{177}Lu-PP-F11N with SG and without kidney protection in the same patient in a random crossover order.

MATERIALS AND METHODS

Study Design and Patients

This was a prospective, randomized, crossover phase 0 single-center study (ClinicalTrials.gov: NCT02088645). The study is part of a project aiming to clinically evaluate ^{177}Lu-PP-F11N in patients with medullary thyroid cancer (Lumed study) approved by the ethics committee of Nordwest and Central Switzerland, and all patients signed a written informed consent form in accordance with the Declaration of Helsinki.

The main inclusion criteria were histologically confirmed MTC with or without thyroidectomy and either elevated levels of calcitonin (>100 pg/mL; >29.2 pmol/L) or a calcitonin doubling time of less than 24 mo. Patients who had received vandetanib less than 3 wk before the study and patients with reduced kidney or bone marrow function (calculated glomerular filtration rate: <60 mL/min/1.73 m^2 of body surface; thrombocytes: <70,000/μL; leukocytes: <2,500/μL; hemoglobin: <8 g/dL) were not included.

Preparation of ^{177}Lu-PP-F11N

^{177}Lu-PP-F11N was produced according to good manufacturing practice (GMP) by the Paul Scherrer Institute, Villigen, Switzerland. The precursor peptide, PP-F11N (2,031.5 g/mol; GMP-grade quality; piCHEM GmbH), carries on its N-terminal end a DOTA moiety that allows stable chelation of ^{177}Lu. GMP-grade no-carrier-added ^{177}LuCl$_3$ (EndolucinBeta) was provided by ITG Isotope Technologies Garching GmbH. Radiolabeling of PP-F11N was done in a synthesis module (PharmTracer; Eckert & Ziegler). The reaction mixture, composed of 100 μg of PP-F11N in aqueous 0.25 M ammonium acetate buffer (pH 5.5) (trace pure reagents; Sigma Aldrich) and sodium ascorbate (United States Pharmacopeia grade), was incubated for 40 min at 60°C with 1.7 GBq of EndolucinBeta. The reaction mixture was purified with a C18 SepPak column (Waters Corporation), and then sterile filtration into a bulk vial was done. The bulk product contained 20.9 mL of 0.9% saline, 1.25 mL of ethanol, 1.75 mL of water for injection, 0.1 mL of DTPA (200

mg/mL), 250 mg of sodium ascorbate, and ^{177}Lu-PP-F11N (total volume of 24 mL). After the material was dispensed via a second sterile filter and aliquots were taken for quality control, the resulting product vial contained 20 ± 2 (mean ± SD) mL of the final product tested for compliance with specifications (radiochemical purity: ≥95%; ^{177}Lu-DTPA: ≤2%; peptide content: <100 μg of total PP-F11N; endotoxins: ≤175 endotoxin units). The product contained about 1 GBq of radioactivity at the end of the shelf life of 24 h.

Injection

Patients received about 1 GBq of ^{177}Lu-PP-F11N with and without SG in a random crossover order within 4 wk. The administration of SG (Gelofusine) was performed in accordance with the International Atomic Energy Agency–European Association of Nuclear Medicine–Society of Nuclear Medicine and Molecular Imaging guideline for peptide receptor radionuclide therapy (18), starting with a bolus dose of 6 mL/kg of body weight/min 10 min before the start of the injection of ^{177}Lu-PP-F11N. After termination of the ^{177}Lu-PP-F11N infusion, the SG infusion was continued at a lower rate of 0.02 mL/kg of body weight/min for 3 h.

Vital signs were recorded for 24 h, and a 12-lead electrocardiogram was obtained before and 2 h after each injection. Clinical laboratory tests (hematology and biochemistry) were assessed until 12 wk after the second injection. Adverse events were recorded and graded according to Common Terminology Criteria for Adverse Events (CTCAE) version 4.03.

Biodistribution, Pharmacokinetics, and Dosimetry

Whole-body planar imaging and SPECT from neck to pelvis were performed on a calibrated SPECT/CT scanner (Symbia Intevo; Siemens Medical Solutions) 1, 4, 24, and 72 h after injection. Combined SPECT/CT was performed 24 h after injection with low-dose nonenhanced CT (130 kVp; 40 mAs) for attenuation correction, anatomic reference, and measurement of tumor diameters. The SPECT/CT scanner was equipped with a medium-energy, parallel-hole collimator and was calibrated to a ^{75}Se source (Siemens Medical Solutions). Image acquisition was done with 2 detectors: 180° of rotation per detector, 64 projections per detector, 20 and 24 s (late scan at 72 h) per projection, and a 128 × 128 matrix. The energy windows were set to 208 and 113 keV with a window width of 20%. After data acquisition in the list mode, a prototype version of xSPECT Quant (Siemens Medical Solutions) was used for ^{177}Lu quantification to obtain attenuation- and scatter-corrected quantitative datasets for 3-dimensional dosimetry studies.
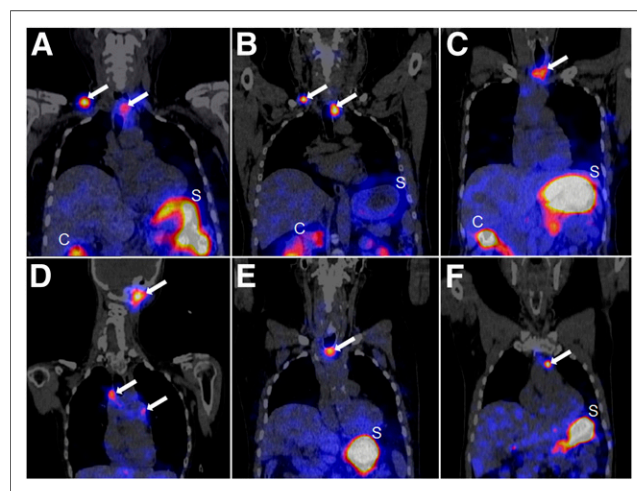

FIGURE 1. ^{177}Lu-PP-F11N SPECT/CT scans in coronal orientation 24 h after injection. In all 6 patients (patients 1–6 [A–F, respectively]), several tumors were visualized with SPECT (white arrows). Minimal diameter of detectable tumor was 8 mm (patient 6 [F]). C = colon; S = stomach.
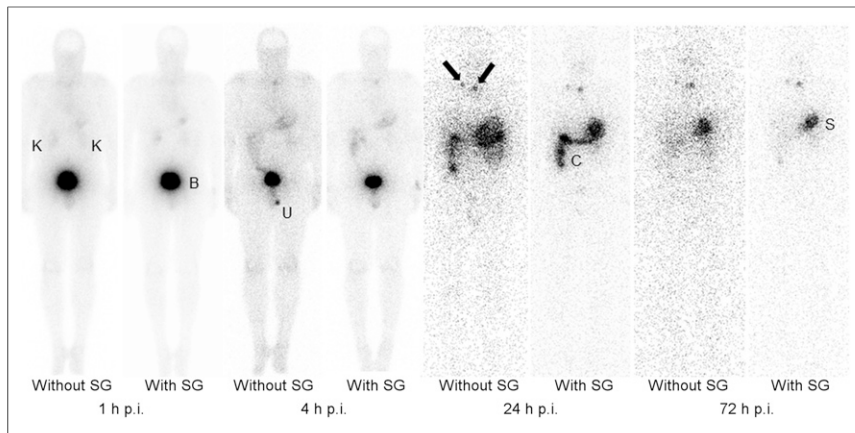
FIGURE 2. Planar scans (anterior view) of patient 2 without and with coadministration of SG at 1, 4, 24, and 72 h after injection (p.i.) of 1 GBq of ^{177}Lu-PP-F11N. On planar scans, 2 tumors with diameters of 10 × 10 mm and 7 × 18 mm (black arrows) were visible. B = urinary bladder; C = colon; K = kidneys; S = stomach; U = urine contamination.

Fresh frozen tissue samples from 1 patient were available for in vitro autoradiography. In vitro CCK2R autoradiography was performed as described before (7). The sections were incubated with ^{111}In-labeled PP-F11N (45 MBq/nmol) at $6 × 10^5$ cpm/mL. For the assessment of nonspecific binding, an adjacent section of the same specimen was incubated in a tracer solution containing, additionally, 200nM nonradioactive human gastrin (Bachem). The slides were then exposed to Biomax MR films (Carestream Health) for 4 d. For signal quantification, a separate calibration curve based on standard samples containing known amounts of radioactivity was recorded for each experiment. Subsequently, the autoradiograms were analyzed using MCID software (InterFocus). For histopathologic evaluation and localization of the autoradiographic signal, adjacent slices were stained with hematoxylin–eosin.

Dosimetry of tumors, the stomach, and kidneys with and without coadministration of SG was performed with Siemens Dosimetry Research Tool software version 5.4 (Siemens Medical Solutions). This software enables 2 methods for calculation of the radiation dose: a voxel-based 3-dimensional dose kernel approach and a volume-based MIRD procedure using quantitative SPECT/CT datasets with volumes of interest to create a time–activity fit (19). In our study, the more established volume-based MIRD procedure was used.

Tumors with ^{177}Lu-PP-F11N–positive results were identified on SPECT and correlated with CT images. Afterward, tumor volumes of interest were drawn on the basis of the CT volume. For kidney dosimetry, volumes of interest were defined on CT images by an automated segmentation algorithm. If necessary, contours were corrected manually, excluding the renal calices. Dosimetry of the stomach was hindered by stomach movement. To overcome this problem, a conservative measurement was chosen: a volume of interest with a constant volume per patient (median: 3.8 mL; range: 1.9–25.6 mL) was placed over the stomach wall at the level of the maximum uptake across all time points to obtain residence time values (time–activity fit) of the stomach wall. Residence time values of the stomach wall, kidneys, and tumors were multiplied by S values (Monte Carlo simulations) and corrected for effective volumes. Tumor radiation doses were corrected for the partial-volume effect using recovery coefficients. Recovery coefficients were obtained by measurement of a National Electrical Manufacturers Association NU 2007 phantom with a known activity concentration inside spheres of various diameters (the smallest diameter was 10 mm, which corresponds to a sphere of 0.52 cm^3). Recovery coefficients for tumor volumes lying between the measured sphere volumes were estimated by linear interpolation.

OLINDA/EXM 1.0 software (Vanderbilt University) was used for the radiation dose calculations for the large intestine, bladder, and red bone marrow (supplemental data; supplemental materials are available at http://jnm.snmjournals.org). This 2-dimensional method is based on planar images or blood sampling using a blood-to-red marrow activity concentration ratio of 1, as recommended by the European Association of Nuclear Medicine (20).

Standard for Comparison

^{177}Lu-PP-F11N SPECT/CT scans were compared with either ^{18}F-DOPA PET/CT scans or histology, including in vitro autoradiography. ^{18}F-DOPA PET with contrast-enhanced CT was performed 29–36 min after the injection of ^{18}F-DOPA (2.1–4.6 MBq/kg), in accordance with European Association of Nuclear Medicine guidelines (21), without carbidopa pretreatment in a time interval ranging from 7 mo before until 3 mo after the first ^{177}Lu-PP-F11N scan was performed.

Statistical Analysis

All variables were analyzed descriptively. A paired sign test, with a P value of less than 0.05 denoting statistical significance, was used to compare results obtained with SG and without SG (matched pairs).
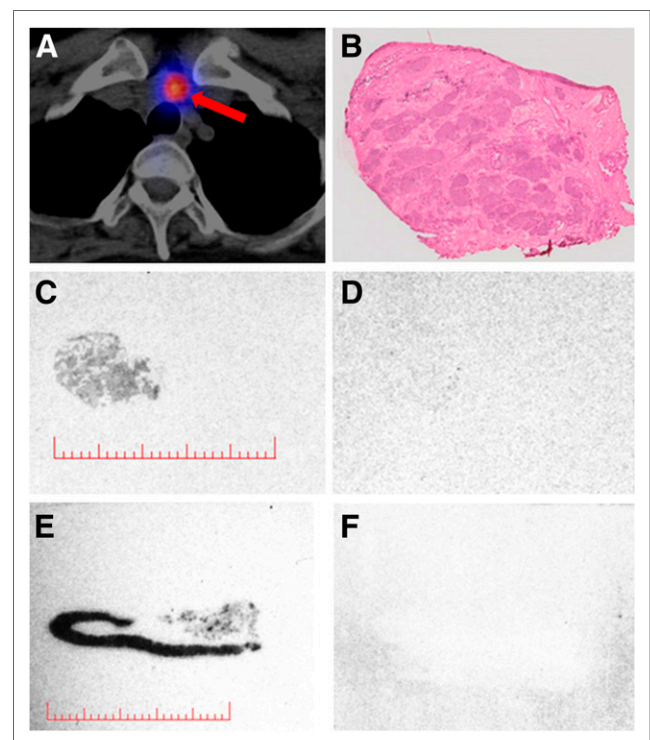

FIGURE 3. (A–D) Images from patient 3 showing axial ^{177}Lu-PP-F11N SPECT/CT scan (A) of suspicious lymph node (red arrow), corresponding tissue stained with hematoxylin–eosin (B), and in vitro autoradiograms of adjacent sections indicating total binding of ^{111}In-PP-F11N (C) and nonspecific binding (D). (E and F) Dog stomach tissue as positive control. Lesion (9 × 9 mm) with uptake on SPECT/CT scan (A) corresponds to lymph node metastasis with 60% tumor cells (B) and specific ^{111}In-PP-F11N binding (C). Red bars = 10 mm. Additional series are shown in Supplemental Figure 1.

RESULTS

Patients

Six consecutive patients with histologically proven MTC were screened and participated in the study. They all completed the study and were included in the proof-of-principle, safety, pharmacokinetic, and dosimetry evaluations. All patients had had a thyroidectomy. Further baseline demography and disease characteristics are shown in Supplemental Table 1.

Proof of Principle

After the infusion of $1,040 \pm 70$ MBq (range: 915–1,226 MBq) of ^{177}Lu-PP-F11N, focal uptake concordant with pathologic lesions was visible on whole-body scintigraphy and SPECT/CT in all patients (Figs. 1 and 2). The median volume of the tumors that underwent dosimetry was 0.72 cm^3 (interquartile range [IQR]: 0.57–1.51). Comparison with ^{18}F-DOPA PET/CT in 4 patients and with histology in 2 patients confirmed tumor-specific ^{177}Lu-PP-F11N accumulation in all patients. Lesions identified by ^{177}Lu-PP-F11N SPECT/CT showed good correlation with those identified by ^{18}F-DOPA PET/CT, as 41 of 49 lesions with positive ^{18}F-DOPA results had positive ^{177}Lu-PP-F11N results, too. On resected lesions from patient 3, in vitro autoradiography performed with ^{111}In-PP-F11N and histologic assessment showed proof of tumor-specific,

CCK2R-mediated ^{177}Lu-PP-F11N accumulation in lymph node metastases (Fig. 3). One lymph node metastasis with a maximum diameter of 8 mm and 40% tumor involvement was not visible with SPECT/CT but showed specific and intense ^{111}In-PP-F11N uptake in vitro (Supplemental Fig. 1). The minimal size of the tumors detectable with SPECT/CT was 8 mm (Fig. 1).

Safety, Pharmacokinetics, and Dosimetry

The short infusion (duration range: 4–6 min) of 79.3 ± 10.5 μg (range: 67.0–94.5 μg) of ^{177}Lu-PP-F11N was well tolerated, with only grade 1 toxicity (Table 1).

Blood sampling for ^{177}Lu-PP-F11N revealed biexponential blood clearance with α-phase half-lives of 11 ± 3.3 min (with SG) and 10.8 ± 5.4 min (without SG) and β-phase half-lives of 162 ± 12 min (with SG) and 163 ± 14 min (without SG); approximately 45% of the administered activity was cleared in the α-phase. SG infusion starting 10 min before the injection of ^{177}Lu-PP-F11N did not significantly reduce the renal absorbed dose; the median absorbed doses were 0.11 (IQR: 0.07–0.13) Gy/GBq without SG and 0.06 (IQR: 0.05–0.09) Gy/GBq with SG ($P = 0.38$; 2-sample paired sign test). The small amount of absorbed dose to the kidneys indicated low retention of ^{177}Lu-PP-F11N in the kidneys despite its predominant renal excretion (Fig. 2). The highest absorbed doses were determined for tumors and the stomach; the median absorbed

TABLE 1
Adverse Events (AE) Observed After Injection of ^{177}Lu-PP-F11N

Patient	AE without SG	AE with SG	Relationship
1	Hot flashes	Hot flashes	Probable
2	Hot flashes	Hot flashes	Probable
	Nausea and vomiting	Nausea and vomiting	Probable
	Paresthesia	Paresthesia	Probable
	Toothache	Toothache	Probable
		Hypotension	Probable
	Fatigue		Possible
	Headache		Possible
3	Numbness		Probable
	Hypotension	Hypotension	Probable
4	Nausea and vomiting	Nausea and vomiting	Probable
	Tachycardia		Probable
		Hypotension	Possible
	Hypocalcemia		Possible
		Fatigue	Probable
		Hypokalemia	Probable
5		Hot flashes	Probable
	Hypocalcemia	Hypocalcemia	Probable
		Hypokalemia	Possible
	Nausea	Nausea	Probable
	Abdominal pain	Dizziness	Probable
			Possible
6	Hypotension	Hypotension	Probable
	Hypokalemia		Possible

Intensity was graded in accordance with CTCAE version 4.03. All events were grade 1 intensity.

doses without SG were 0.88 (IQR: 0.85–1.04) Gy/GBq for tumors and 0.42 (IQR: 0.25–1.01) Gy/GBq for the stomach, resulting in a median tumor-to-stomach dose ratio of 3.34 (IQR: 1.14–4.70) (Table 2). Blood sampling revealed comparable median bone marrow doses with and without SG (0.032 and 0.028 Gy/GBq, respectively) (Table 2). A summary of the dosimetry results for all of the organs is given in Supplemental Table 2.

DISCUSSION

The 5 main findings of this phase 0 clinical trial can be summarized as follows: ^{177}Lu-PP-F11N showed specific accumulation with a sufficiently high radiation dose in MTC tissue, potentially allowing a therapeutic approach; in vitro data from autoradiography were consistent with in vivo data; acute toxicity of ^{177}Lu-PP-F11N was low; dosimetry results suggested that the dose-limiting organ was the stomach; and the coadministration of SG did not affect the tumor-to-kidney dose ratio.

Even though the injected activity was low (1 GBq), ^{177}Lu-PP-F11N SPECT/CT imaging detected lesions in all patients. Forty-one of 49 lesions with positive ^{18}F-DOPA PET/CT results could also be identified with SPECT imaging; the smallest detected metastasis measured only 8 mm, confirming effective CCK2R targeting and low background activity with ^{177}Lu-PP-F11N. In 1 lesion with negative ^{177}Lu-PP-F11N SPECT results, in vitro autoradiography showed ^{111}In-PP-F11N–specific accumulation in an 8-mm lymph node metastasis with 40% tumor infiltration. This example showed that even small metastases with negative SPECT results could be treated with ^{177}Lu-PP-F11N. The tumor radiation doses calculated in the present study were lower than those normally calculated for radionuclide therapy with ^{177}Lu-labeled somatostatin receptor subtype 2–specific ligands in patients with non-MTC neuroendocrine tumors. For example, the median tumor dose for ^{177}Lu-PP-F11N in the present study was 0.88 Gy/GBq, whereas that for ^{177}Lu-DOTATATE in neuroendocrine tumors was 2.0 Gy/GBq (22). On the other hand, in vitro autoradiography studies have shown a higher incidence of CCK2R than of SST2R expression in MTC; a ^{125}I-labeled CCK2R agonist showed specific binding in greater than 90% of MTC, whereas a ^{125}I-labeled SST2R agonist showed specific binding in less than 30% of MTC (7,23). Furthermore, the radiation doses to organs such as the kidneys and bone marrow were at least 3 times lower with ^{177}Lu-PP-F11N than with ^{177}Lu-DOTATATE (22). On the basis of our dosimetry study, fractionated treatment with a cumulative activity of 50 GBq of ^{177}Lu-PP-F11N should be possible without surpassing the maximum tolerated dose to the stomach, which has been estimated to be 50 Gy on the basis of external-beam radiotherapy studies (24). Indeed, the third quartile of the ^{177}Lu-PP-F11N absorbed dose to the stomach was 1 Gy/GBq. A cumulative activity of 50 GBq could result in a mean absorbed tumor dose of 50×0.9 Gy ($\sim$45 Gy) or 50×3.6 Gy ($\sim$180 Gy) for patient 2, who showed the highest tumor absorbed dose.

Acute toxicity after the injection of 67.0–94.5 μg of ^{177}Lu-PP-F11N was low and within the range of adverse reactions known from the CCK2R agonist pentagastrin (calcitonin stimulation test) or other minigastrin analogs (8). Radiation-induced toxicity was not observed after treatment with a cumulative activity of approximately 2 GBq of ^{177}Lu-PP-F11N.

TABLE 2
Absorbed Radiation Doses of ^{177}Lu-PP-F11N in Tumors, Kidneys, Stomach, and Bone Marrow Without and With Coadministration of SG

Patient	Mean tumor dose (Gy/GBq)/patient		Mean kidney dose (Gy/GBq)/patient		Stomach dose (Gy/GBq)		Bone marrow dose (Gy/GBq)		Tumor-to-kidney dose ratio		Tumor-to-stomach dose ratio		Tumor-to-bone marrow dose ratio	
	Without SG	With SG	Without SG	With SG	Without SG	With SG	Without SG	With SG	Without SG	With SG	Without SG	With SG	Without SG	With SG
1	1.09	1.04	0.15	0.11	0.45	0.50	0.022	0.025	7.27	9.45	2.42	2.08	49.6	41.6
2	3.59	1.42	0.13	0.07	0.38	0.47	0.025	0.028	27.6	20.3	9.45	3.02	143.6	50.7
3	0.90	0.67	0.06	0.05	1.66	1.46	0.028	0.031	15.0	13.4	0.54	0.46	32.1	21.6
4	0.85	0.64	0.08	0.10	0.20	0.18	0.044	0.039	10.6	6.4	4.25	3.56	19.3	16.4
5	0.85	1.03	0.13	0.05	1.2	2.07	0.036	0.039	6.5	20.6	0.71	0.50	23.6	26.4
6	0.63	0.63	0.05	0.05	0.13	0.26	0.028	0.033	12.6	12.6	4.85	2.42	22.5	19.1
Median	0.88	0.85	0.11	0.06	0.42	0.49	0.028	0.032	11.6	13.0	3.34	2.25	27.9	24.0
IQR	0.85–1.04	0.65–1.04	0.07–0.13	0.05–0.09	0.25–1.01	0.31–1.22	0.026–0.034	0.025–0.038	8.11–14.4	10.2–18.6	1.14–4.70	0.90–2.87	19.3–45.2	16.4–37.8
Test for superiority(P)*	0.38		0.38		0.69		0.22		1.0		0.16		0.22	

*Two-sample paired sign test with significance level (α) of 0.05.

Calculated kidney radiation doses were low and resulted in higher median tumor-to-kidney radiation dose ratios than the commonly used therapeutic radiotracer ^{177}Lu-DOTATATE (11.6 vs. 1.6) (22). In contrast to findings obtained with DTPA-Glu[1]-minigastrin (9), the coadministration of SG did not significantly reduce the tumor-to-kidney dose ratio in the present study. Therefore, nephroprotection with SG in combination with ^{177}Lu-PP-F11N is not beneficial and can be omitted, as kidney doses are already low. The stomach received the highest calculated organ radiation dose and therefore most likely is the dose-limiting organ. This finding has been reported for CCK2R ligands before (8) and can be explained by the specific binding of ^{177}Lu-PP-F11N to the CCK2R on neuroendocrine cells in the gastric mucosa, mainly enterochromaffinlike cells (25). Interestingly, stomach radiation doses in our patients were heterogeneous (0.18–2.07 Gy/GBq). The patient with the highest stomach dose (patient 5) had a history of medication with proton pump inhibitors. The patient with the lowest dose (patient 4) received an enteral tube feeding formula. Therefore, it can be speculated that gastric acidity and activity (digestion) might have a relevant effect on stomach uptake. This speculation would be in line with the reported increase in enterochromaffinlike cell density and the thickness of the gastric mucosa after chronic acid suppression by proton pump inhibitors (25). The radiation doses to the remaining organs, including bone marrow, were low; therefore, these organs were not considered to be organs at risk for a therapeutic approach.

Evaluation of various radiolabeled minigastrin derivatives with differences in both the C-terminal peptide–binding moiety and the structural characteristics of the linker revealed that the compounds with 6 D-glutamic acid residues within the amino acid chain are the most promising substances, with a reasonable balance of tumor uptake and decreased kidney reabsorption (11,12,16). The pronounced hydrophilicity of such compounds most likely is the reason for the faster renal excretion and shorter blood half-life of ^{177}Lu-PP-F11N than of ^{177}Lu-DOTATATE (β-phase half-lives of 163 ± 14 and 468 ± 150 min, respectively) (22), resulting in a lower tumor radiation dose. Future strategies to achieve higher tumor doses should be investigated and might involve either increasing tumor uptake (e.g., by upregulation of CCK2R density selectively in MTC) or decreasing stomach uptake (e.g., by a specific diet or manipulation of gastric acidity).

The main limitation of the present study was the small number of evaluated subjects. This limitation might affect the statistical significance of kidney dosimetry with and without SG. However, even if SG has a significant nephroprotective effect, exposing patients to potentially severe SG-related toxicity (i.e., anaphylactic reactions) appears to be unnecessary, as ^{177}Lu-PP-F11N shows low kidney uptake.

CONCLUSION

^{177}Lu-PP-F11N accumulates specifically in MTC lesions, resulting in a radiation dose level that is potentially sufficient for a therapeutic approach. The biodistribution of ^{177}Lu-PP-F11N appears to be favorable, with low kidney and bone marrow radiation doses. The dose-limiting organ most likely is the stomach. Further clinical studies are necessary to evaluate the maximum tolerated dose and efficacy of ^{177}Lu-PP-F11N in MTC and other CCK2R-expressing tumors. The following clinical scenarios should be considered: postoperative adjuvant approach in high-risk patients and palliative treatment of advanced, metastatic disease.

KEY POINTS

QUESTION: Is it possible to target MTC lesions with ^{177}Lu-PP-F11N in humans?

PERTINENT FINDINGS: In a monocentric phase 0 proof-of-principle study, ^{177}Lu-PP-F11N showed low toxicity and specific accumulation in MTC tissue in all 6 included patients.

IMPLICATIONS FOR PATIENT CARE: ^{177}Lu-PP-F11N is a promising and safe radiopharmaceutical for peptide receptor radiotherapy of MTC.

REFERENCES

1. Wells SA Jr, Asa SL, Dralle H, et al. Revised American Thyroid Association guidelines for the management of medullary thyroid carcinoma. *Thyroid.* 2015;25: 567–610.
2. Hadoux J, Pacini F, Tuttle RM, et al. Management of advanced medullary thyroid cancer. *Lancet Diabetes Endocrinol.* 2016;4:64–71.
3. Wells SA Jr, Robinson BG, Gagel RF, et al. Vandetanib in patients with locally advanced or metastatic medullary thyroid cancer: a randomized, double-blind phase III trial. *J Clin Oncol.* 2012;30:134–141.
4. Elisei R, Schlumberger MJ, Müller SP, et al. Cabozantinib in progressive medullary thyroid cancer. *J Clin Oncol.* 2013;31:3639–3646.
5. Iten F, Muller B, Schindler C, et al. Response to [^{90}Y-DOTA]-TOC treatment is associated with long-term survival benefit in metastasized medullary thyroid cancer: a phase II clinical trial. *Clin Cancer Res.* 2007;13:6696–6702.
6. Chatal JF, Campion L, Kraeber-Bodere F, et al. Survival improvement in patients with medullary thyroid carcinoma who undergo pretargeted anti-carcinoembryonic-antigen radioimmunotherapy: a collaborative study with the French Endocrine Tumor Group. *J Clin Oncol.* 2006;24:1705–1711.
7. Reubi JC, Schaer JC, Waser B. Cholecystokinin (CCK)-A and CCK-B/gastrin receptors in human tumors. *Cancer Res.* 1997;57:1377–1386.
8. Behr TM, Béhé MP. Cholecystokinin-B/gastrin receptor-targeting peptides for staging and therapy of medullary thyroid cancer and other cholecystokinin-B receptor-expressing malignancies. *Semin Nucl Med.* 2002;32:97–109.
9. Gotthardt M, van Eerd-Vismale J, Oyen WJ, et al. Indication for different mechanisms of kidney uptake of radiolabeled peptides. *J Nucl Med.* 2007;48:596–601.
10. Béhé M, Kluge G, Becker W, et al. Use of polyglutamic acids to reduce uptake of radiometal-labeled minigastrin in the kidneys. *J Nucl Med.* 2005;46:1012–1015.
11. Ritler A, Shoshan MS, Deupi X, et al. Elucidating the structure-activity relationship of the pentaglutamic acid sequence of minigastrin with cholecystokinin receptor subtype 2. *Bioconjug Chem.* 2019;30:657–666.
12. Laverman P, Joosten L, Eek A, et al. Comparative biodistribution of 12 ^{111}In-labelled gastrin/CCK2 receptor-targeting peptides. *Eur J Nucl Med Mol Imaging.* 2011;38:1410–1416.

13. Kolenc-Peitl P, Mansi R, Tamma M, et al. Highly improved metabolic stability and pharmacokinetics of indium-111-DOTA-gastrin conjugates for targeting of the gastrin receptor. *J Med Chem.* 2011;54:2602–2609.

14. Ocak M, Helbok A, Rangger C, et al. Comparison of biological stability and metabolism of CCK2 receptor targeting peptides, a collaborative project under COST BM0607. *Eur J Nucl Med Mol Imaging.* 2011;38:1426–1435.

15. Fani M, Maecke HR. Radiopharmaceutical development of radiolabelled peptides. *Eur J Nucl Med Mol Imaging.* 2012;39(suppl 1):S11–S30.

16. Sauter AW, Mansi R, Hassiepen U, et al. Targeting of the cholecystokinin-2 receptor with the minigastrin analog ^{177}Lu-DOTA-PP-F11N: does the use of protease inhibitors further improve in vivo distribution? *J Nucl Med.* 2019;60:393–399.

17. Klingler M, Summer D, Rangger C, et al. DOTA-MGS5, a new cholecystokinin-2 receptor-targeting peptide analog with an optimized targeting profile for theranostic use. *J Nucl Med.* 2019;60:1010–1016.

18. Bodei L, Mueller-Brand J, Baum RP, et al. The joint IAEA, EANM, and SNMMI practical guidance on peptide receptor radionuclide therapy (PRRNT) in neuroendocrine tumours. *Eur J Nucl Med Mol Imaging.* 2013;40:800–816.

19. Vija A, Cachovan M. Automated internal dosimetry research tool using quantitative SPECT for the Lu177 theranostic application. *J Nucl Med.* 2017;58(suppl 1):1301.

20. Hindorf C, Glatting G, Chiesa C, et al. EANM Dosimetry Committee guidelines for bone marrow and whole-body dosimetry. *Eur J Nucl Med Mol Imaging.* 2010;37:1238–1250.

21. Bozkurt MF, Virgolini I, Balogova S, et al. Guideline for PET/CT imaging of neuroendocrine neoplasms with ^{68}Ga-DOTA-conjugated somatostatin receptor targeting peptides and ^{18}F-DOPA. *Eur J Nucl Med Mol Imaging.* 2017;44:1588–1601.

22. Wild D, Fani M, Fischer R, et al. Comparison of somatostatin receptor agonist and antagonist for peptide receptor radionuclide therapy: a pilot study. *J Nucl Med.* 2014;55:1248–1252.

23. Reubi JC, Chayvialle JA, Franc B, et al. Somatostatin receptors and somatostatin content in medullary thyroid carcinomas. *Lab Invest.* 1991;64:567–573.

24. Emami B, Lyman J, Brown A, et al. Tolerance of normal tissue to therapeutic irradiation. *Int J Radiat Oncol Biol Phys.* 1991;21:109–122.

25. Barrett TD, Lagaud G, Wagaman P, et al. The cholecystokinin CCK2 receptor antagonist, JNJ-26070109, inhibits gastric acid secretion and prevents omeprazole-induced acid rebound in the rat. *Br J Pharmacol.* 2012;166:1684–1693.